Developmental Biology **232,** 255–264 (2001)
doi:10.1006/dbio.2000.0132, available online at http://www.idealibrary.com on IDEAL®

During Multicellular Migration, Myosin II Serves a Structural Role Independent of its Motor Function

Xiaoxin Susan Xu,*[,1] Eunkyung Lee,* Tung-ling Chen,‡ Edward Kuczmarski,† Rex L. Chisholm,‡ and David A. Knecht*[,2]

**Department of Molecular and Cell Biology, University of Connecticut, Storrs, Connecticut 06269; †Department of Physiology and Biophysics, Chicago Medical School, Chicago Illinois 60064; and ‡Department of Cell and Molecular Biology, Northwestern University Medical School, Chicago, Illinois 60611*

We have shown previously that cells lacking myosin II are impaired in multicellular motility. We now extend these results by determining whether myosin contractile function is necessary for normal multicellular motility and shape control. Myosin from mutants lacking the essential (*mlcE*$^-$) myosin light chain retains the ability to form bipolar filaments that bind actin, but shows no measurable *in vitro* or *in vivo* contractile function. The contractile function is necessary for cell shape control since *mlcE*$^-$ cells, like myosin heavy-chain null mutants (*mhcA*$^-$), were defective in their ability to control their three-dimensional shape. When mixed with wild-type cells in chimeric aggregation streams, the *mlcE*$^-$ cells were able to move normally, unlike *mhcA*$^-$ cells which accumulated at the edges of the stream and became distorted by their interactions with wild-type cells. When *mhcA*$^-$ cells were mixed with *mlcE*$^-$ streams, the *mhcA*$^-$ cells were excluded. The normal behavior of the *mlcE*$^-$ cells in this assay suggests that myosin II, in the absence of motor function, is sufficient to allow movement in this constrained, multicellular environment. We hypothesize that myosin II is a major contributor to cortical integrity even in the absence of contractile function.

Key Words: **myosin; actin; cortex; essential light chain; regulatory light chain; Dictyostelium; motility.**

INTRODUCTION

Cytoplasmic or nonmuscle myosin II is required for the successful completion of several critical cellular functions, including cytokinesis in suspension, cell locomotion, and multicellular morphogenesis. In polarized *Dictyostelium* amoebae and in leukocytes, actin is found in the leading edge, the membrane associated cortex, and the uropod, while myosin is found diffusely throughout the cytoplasm and in the cortex (Fechheimer and Zigmond, 1983; Neujahr *et al.*, 1997). Myosin is not evident in newly extended pseudopods although it can be found in the leading lamella of some cells (Conrad *et al.*, 1989; Verkhovsky *et al.*, 1995).

Supplementary data for this article are available on IDEAL (http://www.idealibrary.com).

[1] Current address: Department of Therapeutic Radiology, Yale University School of Medicine, New Haven, CT 06536.

[2] To whom correspondence should be addressed at U-125, University of Connecticut, Storrs, CT 06269. Fax: (860) 486-4331. E-mail: knecht@uconn.edu.

In nonmuscle cells, myosin II cycles between a Triton-soluble, presumably monomeric, state and a Triton insoluble-state believed to consist of bipolar filaments bound to the actin cortex. In unstimulated *Dictyostelium* cells, about 40% of the myosin II is filamentous (Reines and Clarke, 1985). Following stimulation by the chemoattractant cAMP, the assembly state of myosin changes dramatically, initially becoming more assembled, followed by rapid disassembly (Berlot, 1987; Berlot *et al.*, 1985). In *Dictyostelium*, the extent of myosin assembly and its association with the cortex within the cell is regulated by the phosphorylation state of the myosin heavy chain (Egelhoff *et al.*, 1991, 1993). Mutants that are unable to assemble myosin filaments normally have many of the phenotypic properties of myosin II heavy-chain null mutants, demonstrating the importance of myosin assembly.

In addition to the regulation of myosin heavy-chain assembly by phosphorylation, the light chains play a role in myosin function. The two light chains are associated with the neck region linking the motor domain in the head with the coiled-coil tail. The light chains are believed to contrib-

0012-1606/01 $35.00

ute to the mechanical properties of the neck and thereby to regulate the activity of myosin. Phosphorylation of the RLC increases the actin-activated ATPase activity of myosin and the rate of actin filament movement (Ruppel *et al.*, 1994; Uyeda and Spudich, 1993). *In vivo*, both the ELC and the RLC are required for myosin function (Chen *et al.*, 1994, 1995; Pollenz *et al.*, 1992). Mutations in either the ELC or the RLC can affect myosin ATPase and motor function as assessed by *in vitro* motility assays (Chaudoir *et al.*, 1999; Ho and Chisholm, 1997).

Dictyostelium cells lacking the myosin II heavy chain ($mhcA^-$) are unable to develop beyond the mound stage. It is not clear why cells that can accomplish basic motility and chemotaxis should not be able to accomplish morphogenesis. We hypothesized that movement of cells in a mass of tightly adhered cells has different requirements from movement on a glass or plastic surface. In order to investigate this problem, we developed an assay to assess the ability of mutant cells to move during multicellular development. Mutant cells were labeled with fluorescent dye and then mixed with excess wild-type cells and imaged over time during aggregation. In this chimeric aggregation assay, the mutant cells were found to accumulate at the edges of the streams. This was due to both the inability of the mutants to penetrate into the stream and to their being sorted to the outside. In addition, long cytoplasmic extensions were periodically pulled out from mutant cells as they interacted with wild-type cells in the stream (Shelden and Knecht, 1995). When two cell–cell adhesion systems were eliminated, the $mhcA^-$ cells were now found throughout the stream (Xu *et al.*, 1996). We hypothesized that cortical myosin is necessary for cells to move in this restrictive environment in which they must both apply forces to other cells and resist applied forces. This type of motility would be necessary in other developing systems and also in the movement of immune cells and metastatic cancer cells through various tissue layers.

Myosin can be thought of as having two related activities. In its filamentous form it is both a structural component of the cortex able to crosslink actin filaments and a molecular motor. To investigate the relative contribution of these two activities to multicellular motility, we have taken advantage of mutants that lack both motor and actin-binding function or that lack motor function but are able to assemble and associate with the actin filaments in the cell cortex. While $mhcA^-$ cells lack all myosin function, cells lacking the essential light chain ($mlcE^-$ cells) assemble myosin mini-filaments, but are unable to generate force. Up to 50% of mounds produced following starvation of $mlcE^-$ cells complete multicellular development (Chen *et al.*, 1995), while the development of $mhcA^-$ cells stop at the mound stage (De Lozanne and Spudich, 1987; Knecht and Loomis, 1987).

In this report, we used $mhcA^-$ and $mlcE^-$ cell lines to assess the relative contributions of myosin II actin binding and motor function to cell behavior. Surprisingly, the $mlcE^-$ cells, which lack apparent myosin II motor function, are able to move normally in wild-type aggregation streams. We discuss the hypothesis that, in the cell cortex, ELC^- myosin mini-filaments are able to cross-link actin filaments and stiffen the actin cortex and that this activity is sufficient to allow multicellular motility.

MATERIALS AND METHODS

Cell Lines

Dictyostelium strain NC4A2 is a spontaneous axenic derivative of NC4 and HK321 is a myosin II heavy-chain null mutant derived from NC4A2 (Knecht and Shelden, 1995). JH10 is a thymidine auxotrophic strain (Hadwiger and Firtel, 1992) that is grown in HL5 medium plus 100 mg/ml thymidine. C1 is an essential light-chain mutant in which the essential light-chain ($mlcE^-$) gene is replaced by a thy 1 selectable marker (Chen *et al.*, 1995). All strains except JH10 were grown on plastic Petri dishes in HL5 medium (Sussman, 1987).

Cortical Contraction Assay

The ATP-induced cortical contraction assay was carried out as previously described (Yumura and Fukui, 1985), with minor modifications. Briefly, two days before the experiment, cells were plated on a coverslip in a dish containing HL-5 medium. The coverslip was mounted in a Dvorak Stodtler flow chamber (Nicholson Precision Instruments). The chamber was placed in a stage temperature controller (20/20 Technologies, Inc.) set to 2°C and mounted on the stage of a Zeiss Axiovert microscope. The cells were permeabilized with P buffer (10 mM Pipes, 10 mM EGTA, 1 mM $MgCl_2$, 50 mM KCl, 1 mM DTT, 0.2 mM phenylmethylsulphonyl fluoride, pH 7.6) containing 0.5% Triton X-100 and 0.2 μg/ml rhodamine-phalloidin at 2°C for 10 min. The Triton-resistant cortices were washed by flowing P buffer through the chamber for 5 min and then changing the flow to P buffer containing 1 mM ATP in order to initiate contraction. In order to observe the cytoskeleton contraction, the cytoskeletons were imaged before and during contraction with a 100× 1.30 NA Oil Pol Zeiss Plan neofluar objective using a Biorad MRC-600 confocal laser scanning microscope (CLSM).

Sodium Azide Selection

The sodium azide selection was carried out as previously described (Pasternak *et al.*, 1989; Patterson and Spudich, 1995), with minor modifications. Briefly, two days before the experiments, cells were plated on plastic Petri dishes at low density. The medium was removed and 10 ml of cold selection buffer was added. The selection buffer contained nine parts sterile MCBP buffer (10 mM Na_2HPO_4, 10 mM KH_22PO_4, 2 mM $MgCl_2$, 0.2 mM $CaCl_2$, 0.5 mg/ml dihydrostreptomycin, pH 6.5) and one part HL5 medium. After five minutes of incubation at room temperature, the buffer was removed and cold selection buffer containing 5 μm sodium azide was added to the plate. The plate was placed on a gyratory shaker and 100 μl of sample was collected every two minutes for 30 min. Each sample was placed on a hemocytometer and the cell number was used to determine the number of cells released from the plate.

Stopped-Flow Measurement

The stopped-flow measurement was carried out as previously described (Kuczmarski *et al.*, 1991). Briefly, 5–8 × 10^6 cells were harvested by centrifugation. The cell pellet was resuspended and washed in buffer (100 mM Pipes, pH 6.8, 2.5 mM EGTA, 1 mM $MgCl_2$, 10 mM *N-p*-tosyl argine methyl ester, and 20 mM benzamidine). The cells were resuspended at 10^8 cells/ml in lysis buffer (wash buffer containing 0.5% Triton X-100 and 10 μg/ml leupeptin), washed, and resuspended at 1–5 × 10^8 cytoskeletons/ml. The cytoskeletons were placed in the stopped-flow apparatus at 2 × 10^7/ml and the contraction was measured as an increase in absorbance at 310 nm using a spectrophotometer. The contraction rate was calculated from data obtained during the first few seconds of the reaction, using curve fitting software provided with the spectrophotometer.

Cell Shape in Suspension

Cells were plated in a dish at 5 × 10^5 cells/ml. After 1 day of growth, cells were removed and 1 ml of them was placed in a 50-ml plastic tube. The cells were shaken (200 rpm) for 1 h and then 100-μl aliquots of cells were fixed by mixing with 3 ml of the fixing solution containing 1% glutaraldehyde and 0.1% Triton X-100 in buffer (20 mM KH_2PO_4, 20 mM K_2HPO_4, 2mM $MgSO_4$, 5 mM EGTA, 10 mM Pipes, pH 6.8). The length and width of each cell was measured using the same procedure as previously described (Shelden and Knecht, 1996).

Side View Microscopy

Side view microscopy (SVM) was conducted as previously described (Shelden and Knecht, 1996), with minor modifications. A gel surface was prepared by pouring a mixture of 10% gelatin and 1% agarose in HL5 into a Rose chamber. After hardening, the gel was cut in half with a razor blade and one half was removed. The chamber was turned on its side and cells were plated on the cut edge of the gel. After 10 min, the chamber was returned to its normal orientation, filled with HL-5 media, and incubated for 30 min more before imaging started.

Fields of cells were observed using a Zeiss Axiovert microscope equipped with a 100× 1.3 NA lens and DIC optics. Images were captured using a cooled high-resolution CCD camera (Paultek Imaging) and enhanced with a DSP 2000 video image processor (Dage MTI, Inc.). Images were digitally enhanced and composite images were created using NIH image. The maximum vertical length of each cell was used as a measurement of height, and the site of contact between the cell and the substratum perpendicular to the height was measured as the width.

Synergistic Development with Fluorescently Labeled Cells

Fluorescent labeling of *Dictyostelium* cells was performed as previously described (Knecht and Shelden, 1995). Briefly, cells (2 × 10^6) were harvested from HL-5 medium, washed twice with cold 20 mM KPO_4 buffer (pH 6.5), and resuspended in 100 μl of buffer containing 100 μM 5-chloromethyl-fluorescein diacetate (CMF) (Molecular Probes, Inc.). After being stained at room temperature for 30 min, the cells were pelleted, washed twice with KPO_4 buffer, and resuspended in a final volume of 100 μl KPO_4. Unlabeled cells were harvested from HL-5 medium and washed twice with MCPB buffer. The unlabeled cells were resuspended to a final density of 8 × 10^6 cell/ml. For most experiments, 1.6 × 10^7 unlabeled cells were mixed with 2–3% labeled cells. A 2-ml layer of 1% Noble agar melted in MCPB buffer was added to the observation chamber and 2 ml of cells in MCPB buffer was pipetted onto the agar surface. After the cells attached, excess buffer was removed and the plates were incubated in a humid chamber at 23°C until aggregation began. The chamber was then placed in a stage temperature controller set to 23°C mounted on the stage of a Zeiss Axiovert microscope.

Cells were imaged using a CLSM operated on its low-power setting (25 mW krypton–argon laser attenuated with a 3% neutral density filter). Fluorescence and phase-contrast images for cell localization were collected with a 20 × 0.50 NA Zeiss Plan neofluar phase contrast objective. The brightness and contrast of images were adjusted and in some cases the data were smoothed. The fluorescence data were then subtracted from the phase contrast data and the two images were merged and pseudocolored using locally written software. In some experiments, to assess the dynamic behavior of labeled cells, images were collected at 30-s intervals using the slowest direct scan rate and were transferred to a Power Macintosh 7100/80 computer. The images were merged in the same way as the single image described above and were saved as PICT files and compressed into a time-lapse Quicktime movie.

Two parameters of cell behavior in streams were quantified: the proportion of cells at the edge of the stream and the distortion of cell shape. At 10-frame intervals (5 min) in several different movies, the number of cells having part or all of cell at the outside edge of the stream was determined. This was compared to the total number of labeled cells in the field to determine the proportion excluded to the edge. A distortion was defined as a thin extension of cytoplasm from the cell body longer than 7 μm. This parameter was chosen to distinguish these distortions from normal pseudopods. The proportion of cells in each frame containing distortions was quantified at intervals of 10 frames or more so that the same distortion event was not counted twice.

RESULTS

mlcE$^-$ Mutants Show Reduced Contractile Function

Sodium azide selection distinguishes cells that have myosin II contractile function from those that do not (Pasternak *et al.*, 1989; Patterson and Spudich, 1995). When *Dictyostelium* cells are treated with azide, wild-type cells round up and detach from the surface, while the myosin II heavy-chain–null mutant cells (*mhcA*$^-$) remain adherent (Pasternak *et al.*, 1989). When parental JH10 cells were treated with 5 mM sodium azide, 90.0% of the cells rounded up and detached from the surface within 4 min (Fig. 1). Under the same conditions, only 7.1% of *mhcA*$^-$ cells became detached. When *mlcE*$^-$ cells were treated with azide, 5.0% of the cells detached from the dish. These results indicate that *mlcE*$^-$ cells cannot initiate an azide-induced contraction, suggesting the absence of motor function. A possible explanation for these results might be the decreased association of mutant myosin with the cortex. To test this possibility, the amount of myosin associated with the Triton insoluble ctyoskeleton was measured. The cy-

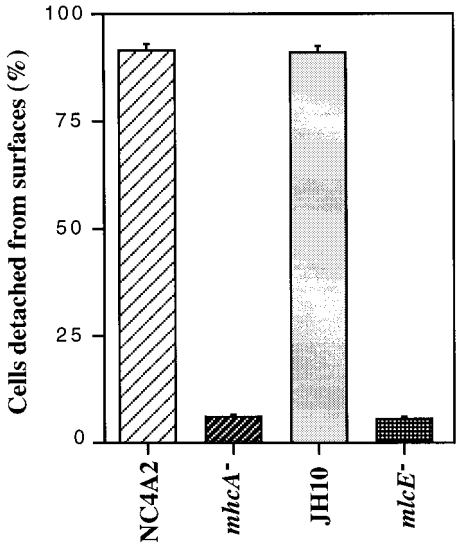

FIG. 1. *mlcE*$^-$ cells do not undergo azide-induced contraction. Cells plated on Petri dishes were exposed to sodium azide and the percentage released 4 min after treatment was counted. Wild-type cells rounded up and detached from the surface while myosin mutant cells (*mlcE*$^-$ and *mhcA*$^-$) remained adhered to the surface.

toskeletons from *mlcE*$^-$ cells contained normal amounts of myosin (data not shown).

A second means of assessing myosin motor function is the direct measurement of cortical contraction. In this assay, Triton-permeabilized wild-type cells contract upon the addition of Mg-ATP while similarly treated *mhcA*$^-$ cells showed no detectable contraction (Fukui *et al.*, 1990). Using this assay, Triton-permeabilized JH10 cells contracted in response to the addition of Mg-ATP. In contrast, there was no contraction of permeabilized *mlcE*$^-$ cells following the addition of ATP (Fig. 2). Contraction can also be measured on a population of cells by following the light-scattering properties of Triton-permeabilized cells using a stopped-flow device (Kuczmarski *et al.*, 1991). In this assay, the cytoskeletal contraction was measured by the increase in absorbance 310 nm after the addition of ATP. The cytoskeletons from *mlcE*$^-$ cells had a less than 5% absorbance change compared to wild-type cells or to their parental cell line (Fig. 3). These results provide independent evidence that cells lacking the ELC have greatly impaired contractile function.

mlcE$^-$ *Cells Show Reduced Vertical Extension*

The above experiments indicate that although myosin lacking light chains is associated with the actin cortex, it is not able to generate contractile tension. Therefore, we were able to assess which aspects of myosin function require contractile activity. One important myosin function is the generation of three-dimensional shape. We found previously that cells lacking myosin are unable to generate shape independent of a substrate or to elongate upward while attached to a substrate (Shelden and Knecht, 1996). It was hypothesized that the generation of shape required a contraction by myosin to reorganize the actin cortex. In order to test this hypothesis, cell shape in mutants lacking the ELC was examined. SVM allows real-time observation of the Z-dimension behavior of cells by culturing them on a surface orthogonal to the optical plane of the microscope. When observed in this way, wild-type cells are normally flattened on the substrate and transiently elongate perpendicular to the substrate. In contrast, *mhcA*$^-$ cells cannot undergo vertical extension and produce only small protrusions on their dorsal surfaces (Shelden and Knecht, 1996). During 30 min of SVM observation, only 1 of 23 *mlcE*$^-$ cells showed some vertical extension (ratio of height/contact area is greater than 1.02) while 9 of 25 wild-type cells became vertically elongated (Fig. 4). Five wild-type cells had a height/contact area ratio greater than 1.6 while no mutant cell showed extensive vertical elongation.

Another way of assessing three-dimensional shape is to view cells in suspension. Wild-type cells can retain their irregular amoeboid three-dimensional shape in suspension while the suspended *mhcA*$^-$ rapidly become spherical (Shelden and Knecht, 1996). When wild-type parental cells (JH10) were viewed in suspension, they had an average length/width ratio of 1.56 ± 0.39 (61 cells) (Fig. 5). In contrast, *mlcE*$^-$ cells showed fewer three-dimensional shape changes than their parental cells and had an average length/width ratio of 1.27 ± 0.22 (n = 63 cells). These results indicate that the binding of mutant myosin to the actin cortex is not sufficient for the generation of three-dimensional cell shape and suggest that motor function is necessary for the vertical extension of cells.

Synergistic Development of mlcE$^-$ *Cells*

Cells lacking the essential light chain are able to complete morphogenesis but form reduced numbers of fruiting bodies. To further investigate the developmental competence of these mutants, the chimeric aggregation assay was used (Knecht and Shelden, 1995). Cells labeled with a fluorescent dye were mixed with unlabeled cells to allow monitoring of the behavior of individual *mlcE*$^-$ cells during development of the chimeras. In this assay, *mhcA*$^-$ cells are typically localized at the edges of wild-type aggregation streams and mounds (Knecht and Shelden, 1995). In addition, *mhcA*$^-$ cells show periodic formation of long cytoplasmic extensions that appear to result when the cortices of the *mhcA*$^-$ cells cannot resist the distention forces applied during adhesive cell–cell interactions (Shelden and Knecht, 1995; Xu *et al.*, 1996) (Fig. 6). In contrast, when labeled *mlcE*$^-$ cells were mixed with wild-type cells, they behaved like wild-type cells, integrating randomly into the streams (Fig. 6C, Table 1). Cytoplasmic extensions were observed only rarely in *mlcE*$^-$ cells. When labeled *mhcA*$^-$ cells were mixed with *mlcE*$^-$ cells, they behaved much as they did in

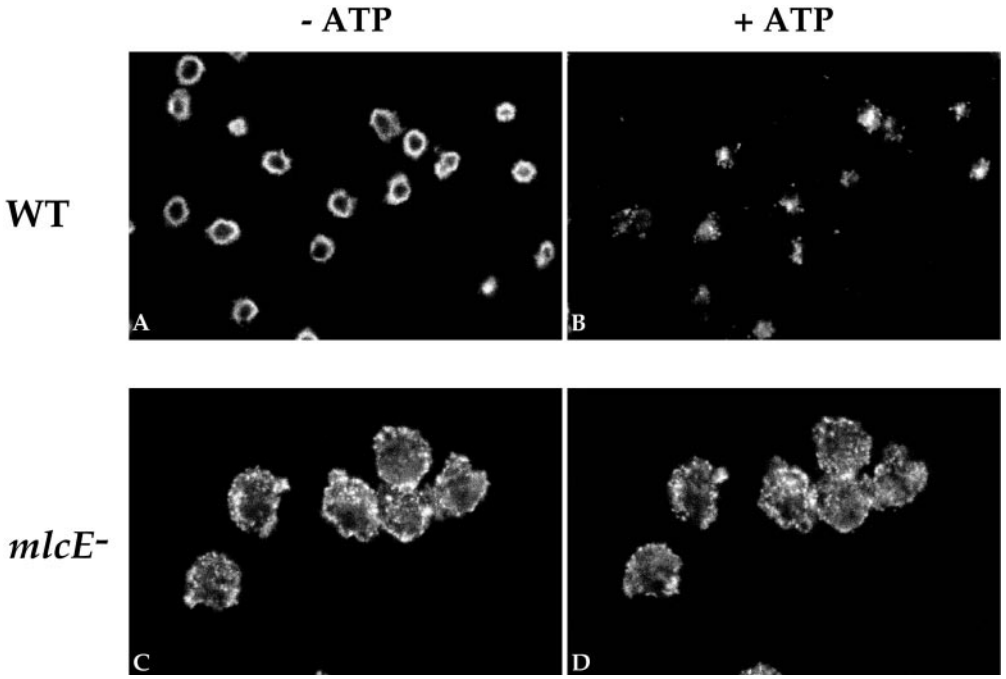

FIG. 2. *mlcE*$^-$ cortices do not undergo ATP-stimulated cortical contraction. Triton-resistant cytoskeletons were isolated in the presence of rhodamine-phalloidin in order to visualize the F-actin cytoskeleton. The isolated cortices were imaged before (A, C) or after (B, D) incubation with ATP. The cytoskeletons of wild-type cells (A, B) contract in the presence of ATP while *mlcE*$^-$ cells (C, D) showed no evidence of contraction.

a wild-type background. The *mhcA*$^-$ cells were seen at the edge of the streams and were distorted by surrounding *mlcE*$^-$ cells (Fig. 6D, Table1). As aggregation proceeds, *mhcA*$^-$ cells that make it into the forming aggregates are found at the periphery of both wild-type and *mlcE*$^-$ mounds (data not shown). Thus *mlcE*$^-$ cells are not only able to penetrate and move normally in aggregation streams made of wild-type cells, but they also are able to exclude *mhcA*$^-$ cells from streams and aggregates.

DISCUSSION

The use of different myosin II mutants allows the role of myosin in different cellular functions to be examined. *mhcA*$^-$ cells contain no myosin II function and are unable to grow in suspension or to develop past the mound stage. In addition, they move at one-third the rate of wild-type cells (Knecht and Loomis, 1987; Wessels *et al.*, 1988). Like *mhcA*$^-$ cells, *mlcE*$^-$ cells are also unable to grow in suspension. About 50% of *mlcE*$^-$ aggregates, however, are able to complete multicellular development. Myosin isolated from *mlcE*$^-$ cells assembles into filaments, binds actin, and disassembles in a normal manner, but lacks actin-activated ATPase activity. The cellular localization and quantity of myosin in *mlcE*$^-$ cells are similar to that in wild-type cells (Chen *et al.*, 1995). The developmental defects exhibited by these mutants indicates that myosin contractile function is required for normal morphogenesis.

Several assays have been used to assess the *in vivo* contractile function of the mutant cell lines. Azide treatment of wild-type cells results in a myosin-driven contraction that causes cells to round up and detach from the surface (Pasternak *et al.*, 1989). In this assay, *mlcE*$^-$ cells behave like *mhcA*$^-$ mutants, remaining attached to the surface (Fig. 1). In a second assay, in which Triton-resistant cytoskeletons were stimulated to undergo a myosin-dependent contraction by the addition of ATP (Yumura and Fukui, 1985), neither *mhcA*$^-$ or *mlcE*$^-$ cytoskeletons contracted. In addition, wild-type cortices were less than half the diameter of those from mutant cells even though the live cells was comparable in size (Fig. 2). A likely explanation for this result is that endogenous ATP causes partial contraction of the wild-type cortices during extraction. Taken together, these observations support the idea that both *mhcA*$^-$ and *mlcE*$^-$ cells lack myosin-dependent contractile function. It has been shown previously that *mlcE*$^-$ cells do not divide when grown in suspension (Chen *et al.*, 1995). Our results show that *mlcE*$^-$ cells are also unable to undergo normal three-dimensional shape changes, either on a surface or in suspension (Figs. 5 and 6). The fact that both *mlcE*$^-$ and *mhcA*$^-$ mutants are incapable of normal shape generation indicates that this behavior requires the motor function of myosin. Similarly, cytokinesis requires three-

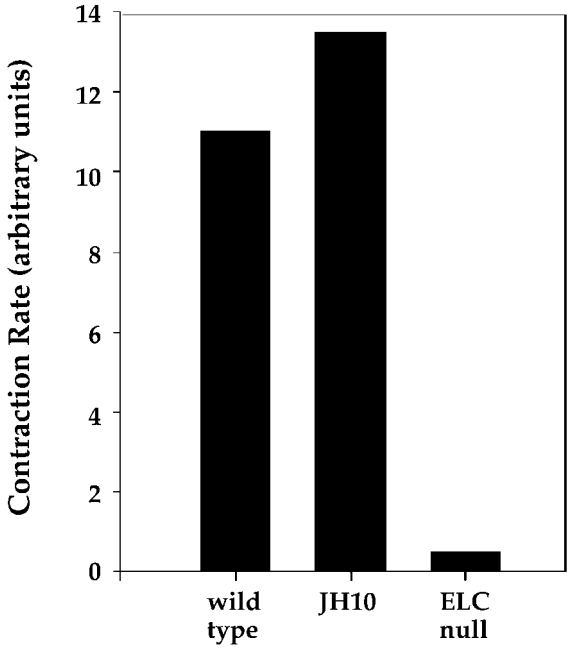

FIG. 3. Rate of ATP-induced contraction. The rate of cytoskeletal contraction in response to ATP was measured spectrophotometrically using a stopped-flow device (25). Cytoskeletons from both *mlcE*$^-$ cells show very low rates of contraction compared to wild-type cells.

dimensional shape control that is dependent on myosin II motor function in order to rearrange the contractile ring.

A chimeric aggregation assay was used to determine the behavior of myosin mutants in a multicellular environment (Knecht and Shelden, 1995). *mlcE*$^-$ cells retained their normal shape and efficiently entered and moved within wild-type aggregation streams while *mhcA*$^-$ cells were excluded. This is in spite of the fact that when analyzed as single cells moving on a glass substrate, both myosin mutants showed similar reductions in their rates of cell movement. Aggregation streams composed of *mlcE*$^-$ cells also excluded *mhcA*$^-$ cells.

The developmental and motility behaviors of these mutants correlates best with myosin assembly and localization. While *mlcE*$^-$ myosin is present at normal levels in the cortex, *mhcA*$^-$ cells have no myosin II in the cortex. Since both myosin mutants lack contractile function by all three assays employed, the differences correlate best with the amount of myosin assembled into the cortex and not with the level of motor function. It is also worth noting that unlike *mhcA*$^-$ cells, *mlcE*$^-$ cells polarize and show normal chemotactic indices during cAMP-induced chemotaxis (Chen *et al.*, 1995, 1998, unpublished observations). In contrast, HMM cells that are unable to assemble their myosin but have normal ATPase activities, show reduced chemotactic index and increased roundness similar to *mhcA*$^-$ cells (Wessels *et al.*, 1988). These results provide

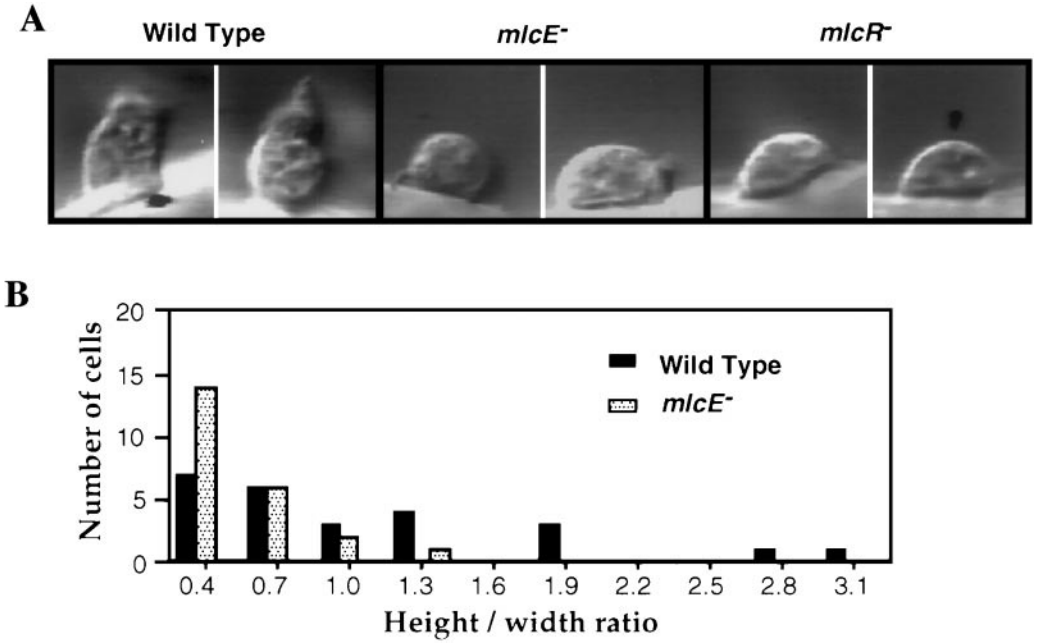

FIG. 4. Observation of cell morphology using side-view microscopy. (A) Gallery of DIC images of cells in the SVM chamber. The cells were cultured on a vertical surface but the images have been rotated to that the substrate is horizontally oriented at the bottom of the image. Wild-type cells (left) periodically become vertically extended away from the substrate. The *mlcE*$^-$ cells (right) remain flattened or hemispherical in shape. (B) Histogram distribution of height/width ratios obtained from wild-type and *mlcE*$^-$ cells.

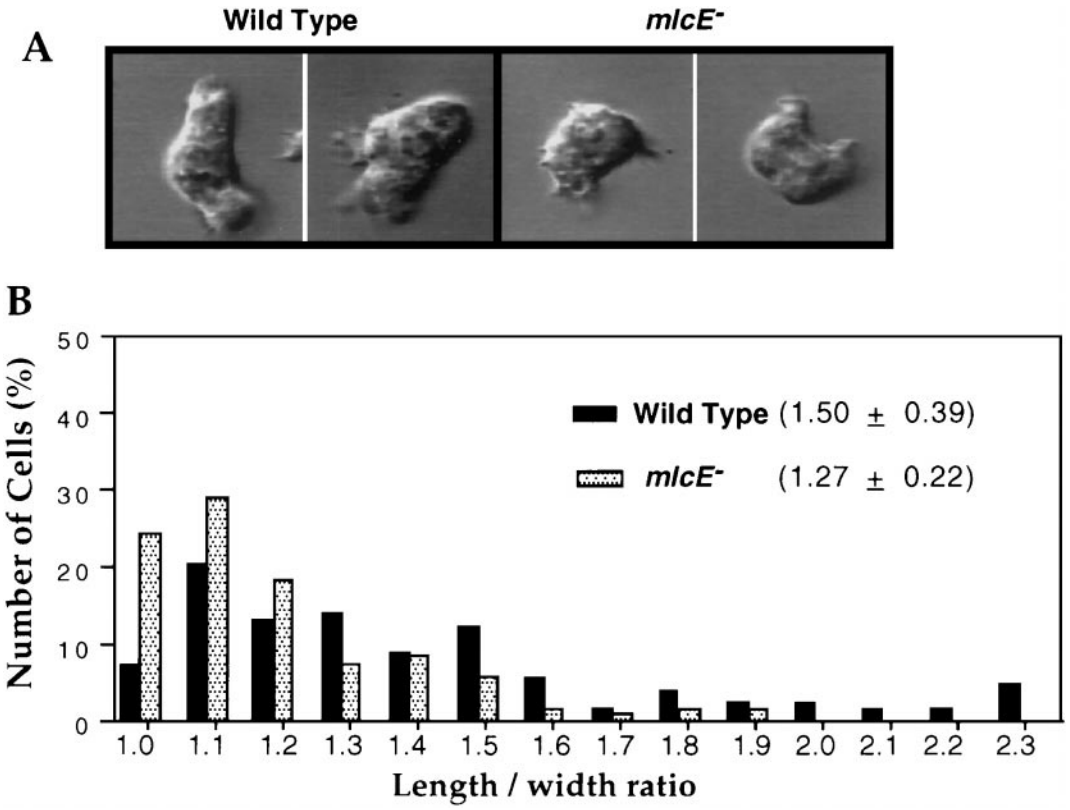

FIG. 5. Morphology of wild-type and myosin mutant cells in suspension. (A) Gallery of DIC images of cells fixed in suspension. Many wild-type cells (left) have an elongated shape. The *mlcE*$^-$ cells have a phenotype that is intermediate between wild-type and *mchA*$^-$ cells (not shown). (B) Histogram of length/width ratios obtained from wild-type and *mlcE*$^-$ cells in suspension.

additional support for the idea that the assembly and cortical localization of myosin filaments, even in the absence of motor function, contribute to the mechanical properties of cells.

Although the *mlcE*$^-$ cells behaved normally during aggregation and mound formation, at later developmental stages most of the *mlcE*$^-$ cells were found at the back of the slug or were left behind on the surface as the slug migrated. These results indicate that while myosin II motor function is not necessary for normal cell behavior during aggregation, it is required for cells to position themselves correctly during later morphogenesis, especially when mutant cells are placed in competition with wild-type cells in chimeric aggregates. When developed on their own, these cells are not fully wild-type even though they form fruiting bodies about 50% of the time (Chen *et al.*, 1995). Therefore, although both motor function and proper cortical association are necessary for normal development, in the absence of motor function a significant portion of the cells can perform morphogenetic movements sufficiently well to complete development.

The surprising result of these experiments is that cells lacking the essential light chain move normally in aggregation streams even though they lack myosin II contractile function. What is the contribution of the *mlcE*$^-$ myosin to the motile behavior of the cells? A significant clue comes from the distortion of *mchA*$^-$ cells by cell–cell interaction in streams. These long cell extensions appear to result when a pulling force is applied to the cell membrane. Wild-type cells resist these forces and the adhesion breaks. In *mchA*$^-$ cells, the membrane and cortex are stretched before the adhesion breaks. We have observed a similar phenomenon with vegetative *mchA*$^-$ cells. As they crawl randomly on plastic surfaces, they often leave behind long, trailing uropods. These tethers eventually detach from the surface and retract into the cell body (D. Knecht, unpublished observations). The stretching of the *mchA*$^-$ cortex in both cases indicates that these cells have trouble maintaining their shape during movement. The stretching could be due to either the increased strength of adhesion or decreased cortical strength. Increased adhesion seems unlikely since the wild-type cells adhering to the *mchA*$^-$ cells should be subjected to equal forces, yet they are not stretched (D. Knecht, unpublished observations). Therefore, decreased cortical strength seems to be the more likely explanation.

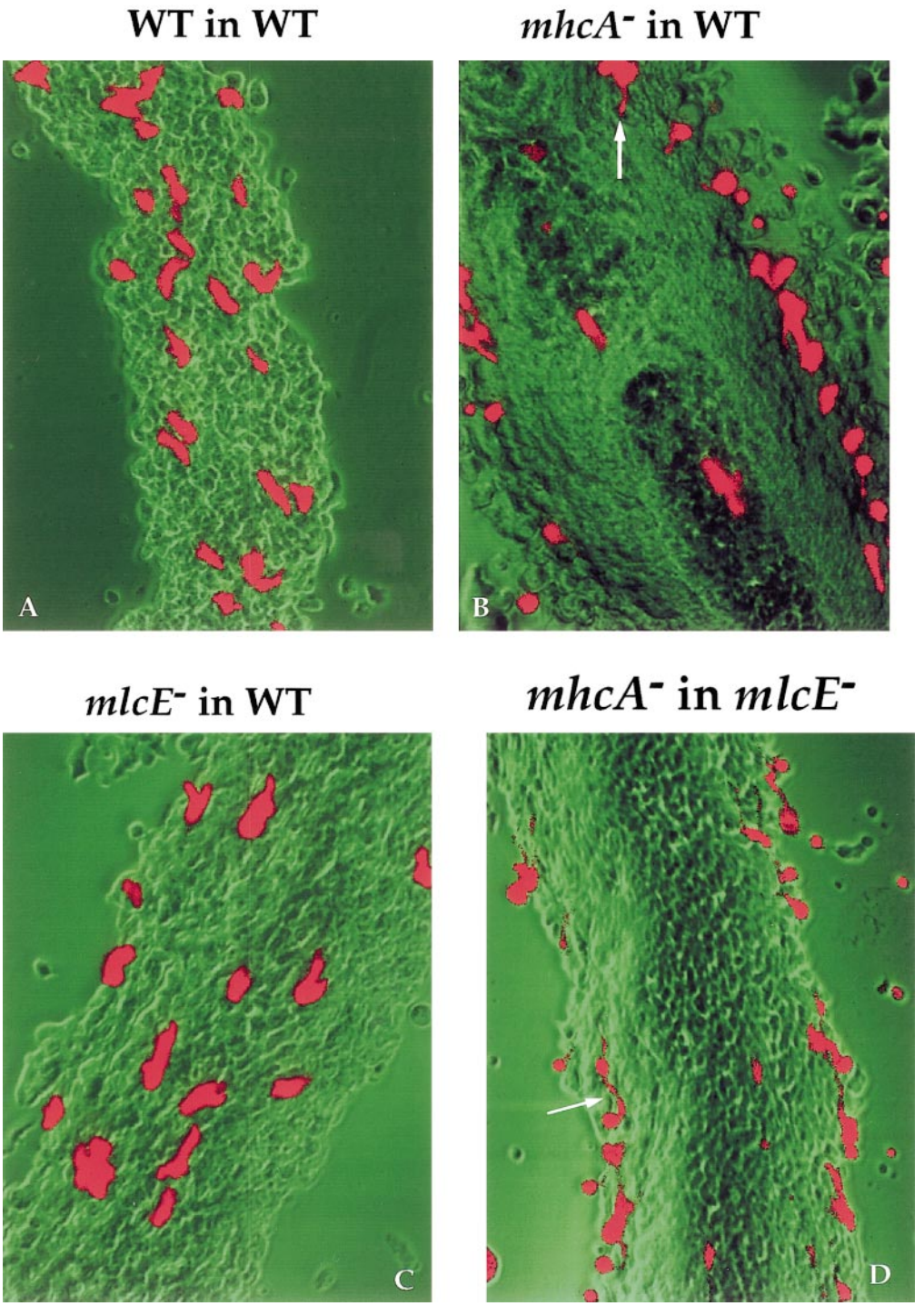

FIG. 6. Distribution of fluorescently labeled wild-type and myosin mutant cells in wild-type aggregation streams. Fluorescently labeled wild-type (A), *mhcA*$^-$ (B), and *mlcE*$^-$ (C) cells were mixed in a 1:50 ratio with unlabeled wild-type cells and plated for development. Fluoresence images and phase-contrast images were captured simultaneously in a single focal plane using confocal microscopy. The images were pseudocolored and merged to show the location of fluorescent cells (red) within the steams (green). *mhcA*$^-$ cells are sorted to the edges of aggregation steams and show long cell extensions (arrow in B). *mlcE*$^-$ cells were indistinguishable from wild-type cells in behavior and location (C). (D) Labeled *mhcA*$^-$ cells were mixed with unlabeled *mlcE*$^-$ cells. The *mhcA*$^-$ cells were sorted to the outside of the aggregation streams and distorted (arrow).

TABLE 1
Behavior of Fluorescently Labeled Cells in Aggregation Streams

	WT in WT	mhcA$^-$ in WT	mlcE$^-$ in WT	mhcA$^-$ in mlcE$^-$
Distorted	5.3% (N = 75)	83.1% (N = 83)	6.0% (N = 67)	38.4% (N = 86)
Edge	26.7% (N = 75)	79.5% (N = 83)	26.9% (N = 67)	79.1% (N = 86)

Note. Quantification of the localization and behavior of fluorescently labeled cells in unlabeled aggregation streams. Fluorescently labeled cells were counted as being at the "Edge" if any part of the cell was at the extreme edge of the stream and as "Distorted" if they contained a thin extension of cytoplasm 7 μm or longer.

Myosin can contribute to cortical stiffness through its motor activity exerting tension on the actin network. Addition of such an active tensioning element to the actin network would result in increased cortical stiffness, as envisioned in tensegrity models (Ingber, 1993). However, the behavior of the *mlcE*$^-$ cells suggests that the presence of bipolar myosin filaments lacking significant motor function stiffens the cortex, perhaps by physically cross-linking actin filaments. Myosin normally produces some cross-linking function since, in order to apply force, multiple heads must always be bound to actin. *mlcE*$^-$ myosin could enter a form analogous to the latch state of smooth muscle (Hai and Murphy, 1988). In this case, myosin would remain bound to actin even in the absence of cycling. What is particularly noteworthy is that mutants lacking ABP-120, which is a major cortical actin cross-linker (Condeelis *et al.*, 1984; Cox *et al.*, 1992), do not show any phenotype in chimeric aggregation streams. Thus myosin II appears to be a more important contributor to cortical integrity than traditional actin cross-linking proteins.

If there is a difference in cortical integrity, then one would like to be able to measure this difference directly; however, such measurements are difficult and crude at present. Measurement of cellular resistance to inward deformation (cell poking) found only a 30% reduction in stiffness in cells lacking the myosin heavy chain (Pasternak *et al.*, 1989). We attempted to deform the cortex of Dictyostelium cells outward with a laser tweezer system by pulling on surface-bound beads. However, in both mutant and wild-type cells, no deformation was possible as the bead pulled out of the trap before the cortex deformed (D. A. Knecht, unpublished observations). As an alternative, we developed an under-agar motility assay to measure the ability of cells to move in a more defined restrictive environment. While wild-type and *mlcE*$^-$ cells can move efficiently under agarose, *mhcA*$^-$ cells are completely unable to move. If the agar concentration is reduced so that the agar is more deformable, *mhcA*$^-$ cells can move under the agar (Laevsky and Knecht, in preparation).

Taken together, these results suggest that the filament assembly and actin-binding activities of *mlcE*$^-$ myosin II are sufficient to allow cells to move in a restrictive environment and to resist applied forces during multicellular movement. Acto-myosin gels assembled *in vitro* can be made to contract but if they are too fluid or too stiff, they do not contract (Condeelis and Taylor, 1977; Janson *et al.*, 1991; Janson and Taylor, 1993).We propose that myosin bound to the cortex is a major contributor to the stiffness and organization of the actin gel. As proposed in the solation–contraction coupling hypothesis (Hellewell and Taylor, 1979), the motor function of myosin II may only come into play when the actin gel is solated, leading to contraction and a change in the overall shape of the cell.

ACKNOWLEDGMENTS

This work was supported by grants from the National Institutes of Health (GM-40599 to D. A. Knecht and GM-39264 to R. Chisholm).

REFERENCES

Berlot, C. (1987). Identification of chemoattractant-elicited increases in protein phosphorylation. *Methods Cell. Biol.* **28,** 333–345.

Berlot, C. H., Spudich, J. A., and Devreotes, P. N. (1985). Chemoattractant-elicited increases in myosin phosphorylation in Dictyostelium. *Cell* **43,** 307–314.

Chaudoir, B. M., Kowalczyk, P. A., and Chisholm, R. L. (1999). Regulatory light chain mutations affect myosin motor function and kinetics. *J. Cell Sci.* **112,** 1611–1620.

Chen, P. X., Ostrow, B. D., Tafuri, S. R., and Chisholm, R. L. (1994). Targeted disruption of the Dictyostelium RMLC gene produces cells defective in cytokinesis and development. *J. Cell. Biol.* **127,** 1933–1944.

Chen, T. L., Wolf, W. A., and Chisholm, R. L. (1998). Cell-type-specific rescue of myosin function during Dictyostelium development defines two distinct cell movements required for culmination. *Development* **125,** 3895–3903.

Chen, T. L. L., Kowalczyk, P. A., Ho, G. Y., and Chisholm, R. L. (1995). Targeted disruption of the Dictyostelium myosin essential light chain gene produces cells defective in cytokinesis and morphogenesis. *J. Cell. Sci.* **108,** 3207–3218.

Condeelis, J., and Taylor, D. (1977). The contractile basis of amoeboid movement. V. The control of gelation, solation, and contraction in extracts from *Dictyostelium discoideum*. *J. Cell. Biol.* **74,** 901–927.

Condeelis, J., Vahey, M., Carboni, J., Demey, J., and Ogihara, S. (1984). Properties of the 120,000-dalton and 95,000-dalton actin-binding proteins from Dictyostelium discoideum and their possible functions in assembling the cytoplasmic matrix. *J. Cell. Biol.* **99,** S119.

Conrad, P., Nederlof, M., Herman, I., and Taylor, D. L. (1989). Correlated distribution of actin, myosin, and microtubules at the leading edge of Swiss 3T3 fibroblasts. *Cell Motil. Cytoskeleton* **14,** 527–543.

Cox, D., Ridsdale, J. A., Condeelis, J., and Hartwig, J. (1995). Genetic deletion of ABP-120 alters the three-dimensional organization of actin filaments in Dictyostelium pseudopods. *J. Cell. Biol.* **128,** 819–835.

De Lozanne, A., and Spudich, J. (1987). Disruption of the Dictyostelium myosin heavy chain gene by homologous recombination. *Science* **236,** 1086–1091.

Egelhoff, T., Brown, S., and Spudich, J. (1991). Spatial and temporal control of nonmuscle myosin localization: Identification of a domain that is necessary for myosin filament disassembly in vivo. *J. Cell. Biol.* **112,** 677–688.

Egelhoff, T. T., Lee, R. J., and Spudich, J. A. (1993). Dictyostelium myosin heavy chain phosphorylation sites regulate myosin filament assembly and localization in vivo. *Cell* **75,** 363–371.

Fechheimer, M., and Zigmond, S. H. (1983). Changes in cytoskeletal protein of polymorphonuclear leukocytes induced by chemotactic peptides. *Cell Motil.* **3,** 349–361.

Fukui, Y., De Lozanne, A., and Spudich, J. A. (1990). Structure and function of the cytoskeleton of a Dictyostelium myosin-defective mutant. *J. Cell. Biol.* **110,** 367–378.

Hadwiger, J. A., and Firtel, R. A. (1992). Analysis of Galpha4, a G-protein subunit required for multicellular development in Dictyostelium. *Genes Dev.* **6,** 38–49.

Hai, C., and Murphy, R. A. (1988). Cross-bridge phosphorylation and regulation of latch state in smooth muscle. *Am. J. Physiol.* **254,** C99–C106.

Hellewell, S. B., and Taylor, D. L. (1979). The contractile basis of ameboid movement. VI. The solation-contraction coupling hypothesis. *J. Cell Biol.* **83,** 633–648.

Ho, G. Y., and Chisholm, R. L. (1997). Substitution mutations in the myosin essential light chain lead to reduced actin-activated ATPase activity despite stoichiometric binding to the heavy chain. *J. Biol. Chem.* **272,** 4522–4527.

Ingber, D. E. (1993). Cellular tensegrity: Defining new rules of biological design that govern the cytoskeleton. *J. Cell. Sci.* **104,** 613–627.

Janson, L. W., Kolega, J., and Taylor, D. L. (1991). Modulation of contraction by gelation/solation in a reconstitued motile model. *J. Cell Biol.* **114,** 1005–1015.

Janson, L. W., and Taylor, D. L. (1993). In vitro models of tail contraction and cytoplasmic streaming in amoeboid cells. *J. Cell Biol.* **123,** 345–356.

Knecht, D., and Loomis, W. (1987). Antisense RNA inactivation of myosin heavy chain gene expression in *Dictyostelium discoideum*. *Science* **236,** 1081–1086.

Knecht, D. A., and Shelden, E. (1995). Three dimensional localization of wild-type and myosin II mutant cells during morphogenesis of dictyostelium. *Dev. Biol.* **170,** 434–444.

Kuczmarski, E. R., Palivos, L., Aguado, C., and Yao, Z. L. (1991). Stopped-flow measurement of cytoskeletal contraction: Dictyostelium myosin II is specifically required for contraction of amoeba cytoskeletons. *J. Cell. Biol.* **114,** 1191–1199.

Neujahr, R., Heizer, C., Albrecht, R., Ecke, M., Schwartz, J., Weber, I., and Gerisch, G. (1997). Three-dimensional patterns and redistribution of myosin II and actin in mitotic Dictyostelium cells. *J. Cell. Biol.* **139,** 1793–1804.

Pasternak, C., Spudich, J. A., and Elson, E. L. (1989). Capping of surface receptors and concomitant cortical tension are generated by conventional myosin. *Nature* **341,** 549–551.

Patterson, B., and Spudich, J. (1995). A novel positive selection for identifying cold-sensitive myosin II mutants in Dictyostelium. *Genetics* **140,** 505–515.

Pollenz, R. S., Chen, T. L. L., Trivinos-Lagos, L., and Chisholm, R. L. (1992). The Dictyostelium essential light chain is required for myosin function. *Cell* **69,** 951–962.

Reines, D., and Clarke, M. (1985). Immunochemical analysis of the supramolecular structure of myosin in contractile cytoskeletons of Dictyostelium amoebae. *J. Biol. Chem.* **260,** 14248–14254.

Ruppel, K. M., Uyeda, T. Q. P., and Spudich, J. A. (1994). Role of highly conserved lysine 130 of myosin motor domain—in vivo and in vitro characterization of site specifically mutated myosin. *J. Biol. Chem.* **269,** 18773–18780.

Shelden, E., and Knecht, D. A. (1995). Mutants lacking myosin II cannot resist forces generated during multicellular morphogenesis. *J. Cell. Sci.* **108,** 1105–1115.

Shelden, E., and Knecht, D. A. (1996). Dictyotelium cell shape generation requires myosin. *Cell. Motil. Cytoskeleton* **35,** 59–67.

Sussman, M. (1987). Cultivation and synchronous morphogenesis of Dictyostelium under controlled experimental conditions. *Methods Cell. Biol.* **28,** 9–29.

Uyeda, T. Q. P., and Spudich, J. A. (1993). A functional recombinant myosin-II lacking a regulatory light chain binding site. *Science* **262,** 1867–1870.

Verkhovsky, A. B., Svitkina, T. M., and Borisy, G. G. (1995). Myosin II filament assemblies in the active lamella of fibroblasts: their morphogenesis and role in the formation of actin filament bundles. *J. Cell. Biol.* **131,** 989–1002.

Wessels, D., Soll, D., Knecht, D., Loomis, W., Delozanne, A., and Spudich, J. (1988). Cell motility and chemotaxis in *Dictyostelium* amebae lacking myosin heavy-chain. *Dev. Biol.* **128,** 164–177.

Xu, X. S., Kuspa, A., D., F., Loomis, W. F., and Knecht, D. A. (1996). Cell-cell adhesion prevents mutants lacking myosin II from penetrating aggregation streams of Dictyostelium. *Dev. Biol.* **175,** 218–226.

Yumura, S., and Fukui, Y. (1985). Reversible cyclic AMP-dependent change in distribution of myosin thick filaments in Dictyostelium. *Nature* **314,** 194–196.

Received for publication June 12, 2000
Accepted December 1, 2000
Published online March 5, 2001